One-Phonon Collision Corrections to the High-Frequency Dielectric Function of Semiconductors

D. E. McCumber
Bell Telephone Laboratories, Murray Hill, New Jersey
(Received 26 August 1966)

Expressions for the one-phonon collision corrections to the high-frequency long-wavelength ($\mathbf{k} \to 0$) dielectric function $\epsilon(\omega)$ of a semiconductor have been computed in the low-temperature cold-electron-plasma limit. Only interactions with a single optical-phonon branch are considered, but expressions for both polar and deformation-potential coupling have been included. Our results differ from previously published work on one-phonon collision corrections in that we have taken dynamic screening into account, a feature which is important when the electron-plasma frequency is comparable to or greater than optical-phonon frequencies. The principal effect of dynamic screening is to replace the noninteracting phonon and electron excitation frequencies in the collision terms with the collective-oscillation frequencies of the interacting electron-phonon system.

I. INTRODUCTION

THE restrictions imposed by energy and momentum conservation are sufficient to preclude the absorption of visible or infrared radiation by "free" electrons in a solid. It is well known that for this reason the long-wavelength high-frequency conductivity of free electrons is purely imaginary and that their contribution to the dielectric function of semiconductors is real and purely reactive. If the conduction electrons are not strictly free but interact with lattice imperfections, different species of mobile charge carriers, or lattice vibrations (phonons), the resulting collisions modify the electron dispersion relation and generate a real or absorptive component $\sigma(\omega)$ in the conductivity $\tilde{\sigma}(\omega)$ and a corresponding imaginary component in the dielectric function $\epsilon(\omega)=4\pi i\tilde{\sigma}(\omega)/\omega$.[1] For example, elastic scattering leads to the well-known Drude expression

$$\tilde{\sigma}(\omega)_{\text{Drude}}=i\epsilon_\infty\omega_{p0}^2/4\pi(\omega+i\nu_c), \tag{1a}$$

for which the real part

$$\sigma(\omega)_{\text{Drude}}=\nu_c\epsilon_\infty\omega_{p0}^2/4\pi(\omega^2+\nu_c^2), \tag{1b}$$

where ϵ_∞ is the high-frequency dielectric constant of the lattice, $\omega_{p0}^2=4\pi e^2n/m\epsilon_\infty$ is a plasma frequency in which e is the charge, n the density, and m the effective mass (here assumed isotropic) of the free electrons, and $\tau\equiv 1/\nu_c$ is a momentum relaxation time. Electron collisions which disperse energy as well as momentum lead to a complex and frequency-dependent collision frequency $\nu_c(\omega)$. In what follows, we are concerned with those collisions of this latter type which involve the dynamically screened interaction of electrons with optical phonons. We assume that only a single optical-phonon branch is important but admit either polar or deformation-potential coupling.

The elementary processes with which we are specifically concerned are illustrated schematically in Fig. 1. Briefly, they are processes in which the absorption of an electric-field quantum (photon) by an electron is accompanied by the emission or absorption (not shown in Fig. 1) of an optical phonon. The energy and momentum of the photon are shared in the final state by the electrons and the vibrating lattice. Although energy is conserved in the final state, it is not necessarily conserved in the virtual intermediate state.

For mathematical simplicity we restrict our discussion to a zero-temperature "cold-plasma" system. We assume that in the initial state the lattice is in its ground state (no phonons excited) and that all electrons have zero momentum ($\mathbf{k}_1=0$ in Fig. 1). Although these assumptions are accurate only if the energy resolution is poor compared to kT and to the electron Fermi energy $\hbar\omega_F$, as it frequently is, the simple closed-form expressions which result are a compensating advantage. The errors involved are often no worse than those implicit in the more common assumption, which we also make, that the optical-phonon frequency ω_0 (or ω_{l0} for longitudinal polar phonons) is sharp and independent of wave number. The cases of greatest interest to us here are those for which $\omega_{p0}\gtrsim\omega_0\gg\omega_F$ and $kT/\hbar$. The con-

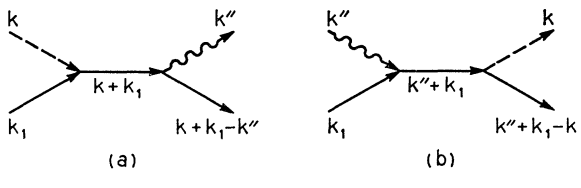

FIG. 1. Schematic representation of some of the elementary single-phonon processes contributing to the conductivity of electrons in a semiconductor. These diagrams show processes in which an electron (solid line) and a phonon (wavy line) share the energy and momentum of an electric-field quantum (dashed line). Diagrams (a) generate positive resistance or loss; diagrams (b) generate negative resistance or gain.

[1] Throughout this paper we use cgs electrostatic units and assume ω real. Our Fourier transforms

$$F(\mathbf{k},\omega)=\int(dr)dt\,f(\mathbf{r},t)\exp(i\omega t-i\mathbf{k}\cdot\mathbf{r})$$

and

$$f(\mathbf{r},t)=(1/V)\,\Sigma_{\mathbf{k}}\int(d\omega/2\pi)F(\mathbf{k},\omega)\exp(-i\omega t+i\mathbf{k}\cdot\mathbf{r}).$$

With these conventions the complex electrical impedance $Z(\omega)=R(\omega)+iX(\omega)$, where R and X are, respectively, resistance and reactance.

dition $\omega_{p0}\gg\omega_F$ implies

$$\frac{\omega_{p0}}{\omega_F}=\frac{(m/m_e)^{1/2}}{\epsilon_\infty^{1/2}(n/n_0)^{1/6}}\gg 1, \tag{2}$$

where $n_0=6.970\times10^{22}$ cm^{-3}. First-order collision corrections to the free-electron conductivity have been numerically computed with dynamic screening by Tzoar[2] for a special case in which ω_F is large: $\omega_F=3.0\omega_{p0}$; $\omega_{p0}=17.8\omega_l$; $\omega_l=10^{13}$ rad/sec.

In the following section we consider collision corrections due to the interaction of electrons with polar phonons. The results show that the principal effect of dynamic screening is to replace the noninteracting phonon and electron excitation frequencies in the collision terms of first-order perturbation theory by the collective-oscillation frequencies of the interacting electron-phonon system. In Sec. III we treat deformation-potential coupling of electrons to phonons and in the last section we briefly indicate the magnitude of the first-order electron-phonon collision corrections in various materials.

II. POLAR PHONONS

In the absence of electron-phonon collisions, but with the Drude contributions (1) included, the long-wavelength high-frequency ($\omega\gg\nu_c$) dielectric function of a polar lattice plus electrons has the form

$$\epsilon(\omega)^0=\epsilon_\infty\left\{\frac{(\omega+i\gamma)^2-\omega_{l0}^2}{(\omega+i\gamma)^2-\omega_t^2}-\frac{\omega_{p0}^2}{\omega^2}\left(1-\frac{i\nu_c}{\omega}\right)\right\}, \tag{3}$$

where ω_t is the angular frequency of the optically active transverse phonons, ω_{l0} the angular frequency of the polar longitudinal phonons in the absence of electrons ($\omega_{p0}=0$), and $\gamma\ll\omega_t$ the damping coefficient of the phonons in a simple Lorentz-line-shape model. If ϵ_0 and ϵ_∞ are, respectively, the low- and high-frequency lattice dielectric constants, the Lyddane-Sachs-Teller relation gives $\omega_{l0}^2=\omega_t^2\epsilon_0/\epsilon_\infty>\omega_t^2$ if $\omega_t\gg\gamma$, as we assume. The real or absorptive part $\sigma(\omega)$ of the conductivity $\tilde{\sigma}(\omega)=\omega\epsilon(\omega)/4\pi i$ computed from (3) has the form ($\omega\gg\nu_c,\omega_t\gg\gamma$):

$$\sigma(\omega)^0=\frac{\epsilon_\infty}{4\pi}\left\{\frac{\omega_{p0}^2}{\omega^2}\nu_c+\tfrac{1}{2}(\omega_{l0}^2-\omega_t^2)\frac{\gamma}{(|\omega|-\omega_t)^2+\gamma^2}\right\}. \tag{4}$$

The last term describes absorption by the optically active Reststrahl bands of the crystal; the first term describes that due to electrons and their Drude collisions.

Gurevich, Lang, and Firsov[3] have computed the first-order collision correction to Eq. (4) resulting from the unscreened interactions of electrons and longitudinal polar phonons. Making the zero-temperature cold-plasma approximations described earlier, we can write their correction to Eq. (4) in the form

$$\Delta\sigma(\omega)=\frac{\alpha\omega_{p0}^2\epsilon_\infty\omega_{l0}^{3/2}}{6\pi|\omega|^3}(|\omega|-\omega_{l0})^{1/2}\theta(|\omega|-\omega_{l0}), \tag{5}$$

where $\alpha=e^2(\epsilon_0-\epsilon_\infty)(m/2\hbar\omega_{l0})^{1/2}/\epsilon_0\epsilon_\infty\hbar$ is the familiar dimensionless polaron coupling coefficient[4] and where the step function

$$\begin{aligned}\theta(x)&=1 \quad \text{for} \quad x>0\\ &=0 \quad \text{for} \quad x<0.\end{aligned} \tag{6}$$

In (5), this step function ensures that no radiation will be absorbed by the cold-electron-lattice system unless [see Fig. 1(a)] it has the minimum energy $\hbar\omega_{l0}$ necessary to excite an optical phonon. The square root in (5) reflects the energy density of conduction-band electron states.

If we neglect the photon momentum ($\mathbf{k}=0$) in Fig. 1(a) and assume that the electrons are initially cold ($\mathbf{k}_1=0$), the final-state phonon and electron momenta are equal and opposite ($\pm\mathbf{k}''$). Equation (5) follows from the additional assumption that the net electron-lattice excitation energy $\Delta E_{fi}(\mathbf{k}'')$, the difference between the final-state and initial-state energies, is

$$\Delta E_{fi}(\mathbf{k}'')=\hbar\omega_{l0}+(\hbar k'')^2/2m\gtrsim\hbar\omega_{l0}. \tag{7}$$

Notice that the electron excitation energy $\Delta E_{fi}(\mathbf{k}'')-\hbar\omega_{l0}$ approaches zero as $k''\to0$. This behavior is only accurate in the limit of vanishing electron density for which $\omega_{p0}\to0$; it is not accurate for ω_{p0} finite. Roughly, if ω_F is small, we expect the long-wavelength electron excitation spectrum to be dominated by the plasma resonance. In that case, the electron system will appear to have a minimum excitation frequency equal to the plasma frequency, and the excitation energy $\Delta E_{fi}(\mathbf{k}'')$ will be bounded below by $\hbar(\omega_{p0}+\omega_{l0})$, such a lower bound being reflected in the step-function cutoff of the absorption spectrum. In their derivation of Eq. (5), Gurevich *et al.*[3] neglected the dynamic screening of the electron-phonon interaction,[5,6] and for this reason their results do not show the expected plasma-frequency effects. When dynamic screening is taken into account, these collective plasma effects correctly appear. Dynamic screening is unimportant if $\omega_{p0}\ll\omega_{l0}$ or if $\omega\gg\omega_{p0}+\omega_{l0}$.

General expressions incorporating the dynamic screening of polar and deformation-potential phonons have been developed elsewhere.[5,6] Specializing those results to a single species of carrier and to a single set

[2] N. Tzoar, Phys. Rev. **133**, A1213 (1964).
[3] V. L. Gurevich, I. G. Lang, and Yu-A. Firsov, Fiz. Tverd. Tela **4**, 1252 (1963) [English transl.: Soviet Phys.—Solid State **4**, 918 (1963)].
[4] H. Fröhlich, Advan. Phys. **3**, 325 (1954).
[5] N. Tzoar, Phys. Rev. **132**, 202 (1963); A. Ron and N. Tzoar, *ibid.* **133**, A1378 (1964).
[6] D. E. McCumber, Rev. Mod. Phys. **38**, 494 (1966).

of infrared-active optical phonons, we find after considerable algebra that the collision correction analogous to (5) for the real or resistive part (4) of the conductivity is

$$\Delta\sigma(\omega)=\frac{\alpha\omega_{p0}^2\epsilon_\infty}{6\pi\omega_{l0}}I_p(|\omega|/\omega_{l0},\omega_{p0}/\omega_{l0},\epsilon_\infty/\epsilon_0)\,, \tag{8a}$$

where

$$I_p(z,x,R^2)=\frac{\{z^2+1-x^2-2[z^2-x^2(1-R^2)]^{1/2}\}^{1/4}\theta(z^2-1-x^2-2xR)}{z^2[z^2-x^2(1-R^2)]^{1/2}}\,. \tag{8b}$$

In the low-density limit for which $x=\omega_{p0}/\omega_{l0}\to 0$,

$$I_p(z,0,R^2)=z^{-3}(z-1)^{1/2}\theta(z-1) \tag{9}$$

and (8a) correctly reduces to (5). The function $I_p(z,x,R^2)$ has been plotted in Fig. 2 as a function of $z=|\omega|/\omega_{l0}$ for various values of $x=\omega_{p0}/\omega_{l0}$ and $R^2=\epsilon_\infty/\epsilon_0$. The absorption threshold, which for fixed ω_{l0} increases as ω_{p0} increases, occurs at a frequency

$$\omega_{\rm th}=(\omega_{l0}^2+2\omega_t\omega_{p0}+\omega_{p0}^2)^{1/2}, \tag{10}$$

which is near the threshold $(\omega_{p0}+\omega_{l0})$ we intuitively estimated. For $z\gg 1$, the function (8b) asymptotically approaches the $x=0$ function (9), so that at high frequencies $(\omega\gg\omega_{l0})$ the collision correction (8a) with dynamic screening approximates the result (5) without screening.

Because the polar phonons and the electrons are coupled through their joint self-consistent electric field,[6] the resonant frequencies of the coupled long-wavelength longitudinal modes are different from ω_{l0} and ω_{p0}, except in special limiting cases.[7,8] In lowest order the frequencies characteristic of longitudinal normal modes of momentum $\mathbf{k}$ are the zeros of the collisionless dielectric function $\epsilon(\mathbf{k};\omega)$[9]. In the cold-plasma system considered here, there are two such modes whose frequencies $\omega_\pm(\mathbf{k})$ satisfy

$$\omega_\pm^2(k)=\tfrac{1}{2}(\omega_{l0}^2+\omega_{p0}^2+\Omega_k^2)\pm\tfrac{1}{2}[(\omega_{l0}^2+\omega_{p0}^2+\Omega_k^2)^2-4(\omega_{l0}^2\Omega_k^2+\omega_{p0}^2\omega_t^2)]^{1/2} \tag{11}$$

with $\Omega_k=\hbar k^2/2m$. In the limit $\omega_{p0}\gg\omega_{l0}$,

$$\omega_+(k)\to[\omega_{p0}^2+\Omega_k^2]^{1/2},$$
$$\omega_-(k)\to[\omega_t^2+(\omega_{l0}^2-\omega_t^2)\Omega_k^2/(\omega_{p0}^2+k^2)]^{1/2}. \tag{12a}$$

In the opposite limit $\omega_{l0}\gg\omega_{p0}$,

$$\omega_+(\mathbf{k})\to\omega_{l0},$$
$$\omega_-(\mathbf{k})\to[\Omega_k^2+\epsilon_\infty\omega_{p0}^2/\epsilon_0]^{1/2}. \tag{12b}$$

In the former case $\omega_-(\mathbf{k})$ belongs to a mode with predominantly phonon character and $\omega_+(\mathbf{k})$ to one with predominantly plasmon character; these characters are reversed in the latter case. In intermediate cases it is less meaningful to identify $\omega_\pm(\mathbf{k})$ as phonon or plasmon frequencies.

While the real part $\sigma(\omega)$ of the conductivity is convenient for physical interpretation, the dielectric function $\epsilon(\omega)$ is generally more relevant to experiments at infrared or visible frequencies. Adding the first-order polar-phonon collision corrections to (3), we find that with dynamic screening the high-frequency $(\omega\gg\nu_c)$ dielectric function is

$$\epsilon(\omega)=\epsilon_\infty\left\{\frac{(\omega^2-\omega_t^2)(\omega^2-\omega_{l0}^2)+\gamma^2[(\omega^2+\omega_t^2)+(\omega^2+\omega_{l0}^2)]+\gamma^4}{(\omega^2-\omega_t^2)^2+2\gamma^2(\omega^2+\omega_t^2)+\gamma^4}-\frac{\omega_{p0}^2}{\omega^2}\left[1+\frac{\alpha}{\pi}\frac{2}{3}P_p(\omega/\omega_{l0},\omega_{p0}/\omega_{l0},\epsilon_\infty/\epsilon_0)\right]\right\}$$
$$+i\epsilon_\infty\left\{\frac{2\omega(\omega_{l0}^2-\omega_t^2)\gamma}{(\omega^2-\omega_t^2)^2+2\gamma^2(\omega^2+\omega_t^2)+\gamma^4}+\frac{\omega_{p0}^2}{\omega^2}\left[\frac{\nu_c}{\omega}+\alpha\frac{2}{3}\frac{\omega}{\omega_{l0}}I_p(|\omega|/\omega_{l0},\omega_{p0}/\omega_{l0},\epsilon_\infty/\epsilon_0)\right]\right\}, \tag{13}$$

where $I_p(z,x,R^2)$ is the function (8b) plotted in Fig. 2 and

$$P_p(z,x,R^2)=2\mathcal{P}\int_0^\infty d\bar{z}\frac{\bar{z}^2I_p(\bar{z},x,R^2)}{z^2-\bar{z}^2}\,. \tag{14a}$$

$\mathcal{P}$ means that the integral in (14a) is the Cauchy principal-value integral. In the low-density limit for which $x=\omega_{p0}/\omega_{l0}\to 0$,

$$P_p(z,0,R^2)=z^{-2}\pi\{(1+|z|)^{1/2}+(1-|z|)^{1/2}\theta(1-|z|)-2\}, \tag{14b}$$

a result previously obtained by Balkanski and Hopfield.[9] The function $P_p(z,x,R^2)$ has been plotted in Fig. 3 as a function of $z=\omega/\omega_{l0}$ for various values of $x=\omega_{p0}/\omega_{l0}$ and

[7] See A. S. Barker, Jr., in *Proceedings of the International Conference on Optical Properties and Electronic Band Structure of Metals and Alloys, Paris, 1965* (North-Holland Publishing Company, Amsterdam, 1966), p. 452.

[8] B. B. Varga, Phys. Rev. **137**, A1896 (1965).

[9] M. Balkanski and J. J. Hopfield, Phys. Status Solidi **2**, 623 (1962).

$R^2=\epsilon_\infty/\epsilon_0$. The sharp cusp in each curve lies at the threshold of the corresponding absorption function $I_p(z,x,R^2)$ of Fig. 2 and results from the rapid rise in $I_p(z,x,R^2)$ at that threshold. The cusps will be blunted by any effects which might soften the absorption edge—for example, the neglected effects of finite temperature and of finite electron Fermi energy.

When $z=x=0$, Eq. (14b) gives $P_p(0,0,R^2)=-\pi/4$, so that in Eq. (13) the factor

$$\omega_{p0}^2[1+(\alpha/\pi)\tfrac{2}{3}P_p]\rightarrow\omega_{p0}^2(1-\alpha/6) \qquad (15)$$

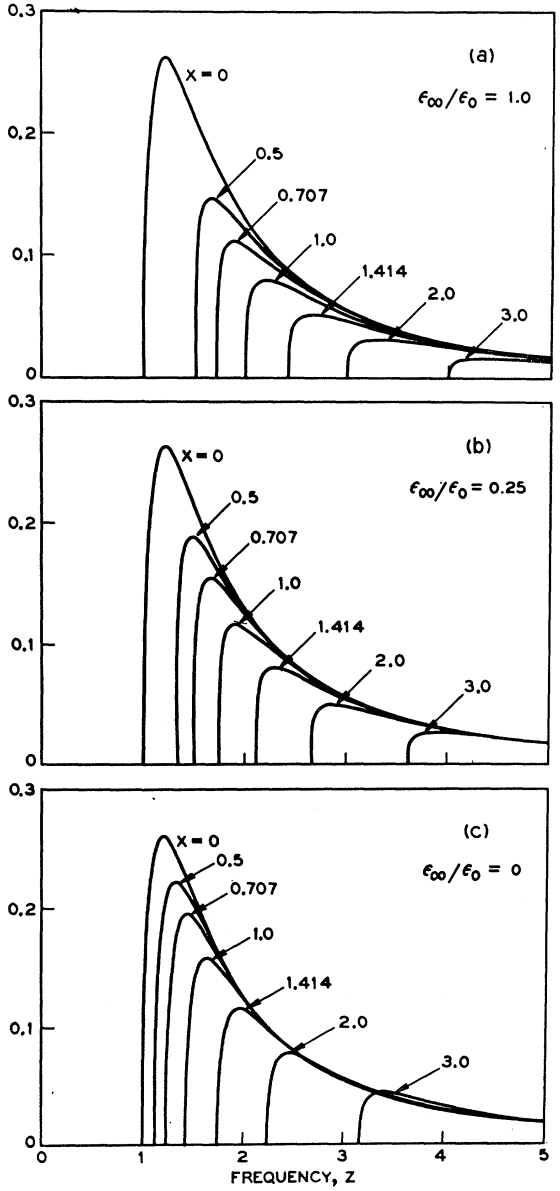

FIG. 2. Polar-phonon collision-correction function $I_p(z,x,R^2)$ as a function of frequency $z=|\omega|/\omega_{l0}$ for different values of $x=\omega_{p0}/\omega_{l0}$ and $R^2=\epsilon_\infty/\epsilon_0$. This function relates to the imaginary or dissipative component of the dielectric function.

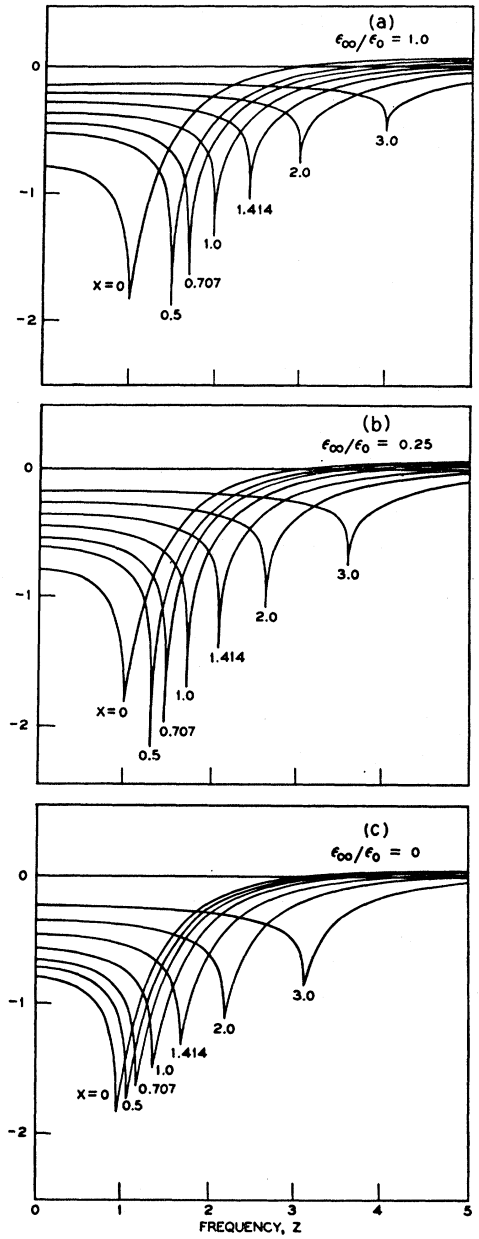

FIG. 3. Polar-phonon collision-correction function $P_p(z,x,R^2)$ as a function of frequency $z=\omega/\omega_{l0}$ for different values of $x=\omega_p/\omega_{l0}$ and $R^2=\epsilon_\infty/\epsilon_0$. This function relates to the real or reactive component of the dielectric function.

in the limit ω, $\omega_{p0}\rightarrow 0$. This limiting result will be recognized as the first-order low-energy polaron correction[4] to the electron mass as it appears in ω_{p0}^2: $m\rightarrow m(1+\alpha/6)$. Figure 3 indicates for ω_{p0} finite ($x>0$) that dynamic screening of the electron-phonon interaction reduces the low-energy ($\omega=0$) polaron mass correction below this single-electron value. For finite frequencies, the "mass correction" varies with frequency in the way indicated by Eq. (13) and Fig. 3.

III. DEFORMATION-POTENTIAL PHONONS

The preceding section pertains to electron collisions with polar phonons. Similar results obtain for electron collisions with deformation-potential-coupled nonpolar phonons, although in this case the transverse phonons are not optically active and the collisionless high-frequency ($\omega \gg \nu_c$) dielectric function (3) has the form

$$\epsilon(\omega)^0=\epsilon_\infty\left\{1-\frac{\omega_{p0}^2}{\omega^2}\left(1-\frac{i\nu_c}{\omega}\right)\right\}. \tag{16}$$

The real or absorptive part of the corresponding conductivity is

$$\sigma(\omega)^0=\frac{\epsilon_\infty}{4\pi}\frac{\omega_{p0}^2}{\omega^2}\nu_c, \tag{17}$$

which is simply the Drude component of (4).

Specializing previously derived general expressions[6] to a single species of carrier and to a single branch of deformation-potential-coupled optical phonons of angular frequency ω_0, we find after considerable manipulation that the collision correction to (17) is

$$\Delta\sigma(\omega)=\frac{E_K^2K^2\omega_{p0}^2}{96\pi^2 m\rho_M}\left(\frac{2m}{\hbar\omega_0}\right)^{5/2} I_d(|\omega|/\omega_0,\omega_{p0}/\omega_0), \tag{18a}$$

where

$$I_d(z,x)=z^{-3}[(z-1)^2-x^2]^{3/4}\theta(z-1-x). \tag{18b}$$

In deriving (18) we have used the phonon-electron interaction due to Seitz[10] in which E_K is a (phenomenological) deformation-potential energy, $\mathbf{K}$ is a vector of the reciprocal lattice, and ρ_M is the mass density of the crystal. We have also assumed, as is nearly always the case, that

$$\gamma_k^2 \ll \omega_0^2+\omega_0^2\Omega_k^2/\omega_{p0}^2 \tag{19}$$

for all k, where $\Omega_k=\hbar k^2/2m$ as in (11) and where

$$\gamma_k^2=E_K^2K^2k^2/4\pi e^2\rho_M. \tag{20}$$

In the low-density limit for which $x=\omega_{p0}/\omega_{l0}\to 0$, $I_d(z,x)$ reduces to

$$I_d(z,0)=z^{-3}(z-1)^{3/2}\theta(z-1), \tag{21}$$

which is the envelope of the finite-x expressions (18b). In Fig. 4 we have plotted $I_d(z,x)$ as a function of $z=|\omega|/\omega_0$ for $x=0$ and for various finite $x=\omega_{p0}/\omega_0$. The

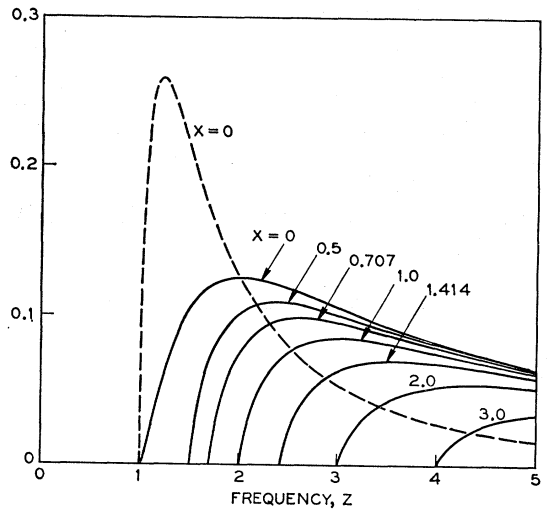

FIG. 4. Deformation-potential-phonon collision-correction function $I_d(z,x)$ as a function of frequency $z=|\omega|/\omega_0$ for different values of $x=\omega_{p0}/\omega_0$. The dashed curve is the polar-phonon function $I_p(z,0,R^2)$ shown previously in Fig. 2 and included here to demonstrate the different spectral shape of the polar and deformation-potential corrections.

absorption threshold in this system occurs at the frequency

$$\omega_{\rm th}=\omega_{p0}+\omega_0, \tag{22}$$

as we would intuitively expect.

Again, because the phonons and the electrons are coupled through a self-consistent field (different from the electric field relevant to polar phonons),[6] it is useful to note the frequencies $\omega_\pm(\mathbf{k})$ of the longitudinal normal modes. In the cold-plasma system considered here,

$$\omega_\pm^2(\mathbf{k})=\tfrac{1}{2}(\omega_0^2+\omega_{p0}^2+\Omega_k^2)\pm\tfrac{1}{2}[(\omega_0^2-\omega_{p0}^2-\Omega_k^2)^2+4\gamma_k^2\omega_{p0}^2]^{1/2}. \tag{23}$$

Near the "crossing" point $\omega_0^2=\omega_{p0}^2+\Omega_k^2$ of the uncoupled modes, the coupled modes have mixed phonon and plasmon character. Away from that point one mode has phonon character and frequency ω_0, while the other has plasmon character and frequency $(\omega_{p0}^2+\Omega_k^2)^{1/2}$.

Adding the first-order deformation-potential phonon collision corrections to (16), we find that with dynamic screening the high-frequency ($\omega \gg \nu_c$) dielectric function analogous to (13) is

$$\epsilon(\omega)=\epsilon_\infty\left\{1-\frac{\omega_{p0}^2}{\omega^2}\left[1+\frac{E_K^2K^2\omega_0}{24\pi^2 m\rho_M\epsilon_\infty}\left(\frac{2m}{\hbar\omega_0}\right)^{5/2}P_d(\omega/\omega_0,\omega_{p0}/\omega_0)\right]\right\}$$
$$+i\epsilon_\infty\frac{\omega_{p0}^2}{\omega^2}\left[\frac{\nu_c}{\omega}+\frac{E_K^2K^2\omega_0}{24\pi m\rho_M\epsilon_\infty}\left(\frac{2m}{\hbar\omega_0}\right)^{5/2}\frac{\omega}{\omega_0}I_d(\omega/\omega_0,\omega_{p0}/\omega_0)\right], \tag{24}$$

[10] F. Seitz, Phys. Rev. 73, 549 (1948); see also J. M. Ziman, *Electrons and Phonons* (Clarendon Press, Oxford, England, 1960), p. 439.

where $I_d(z,x)$ is the function (18b) plotted in Fig. 4 and

$$P_d(z,x)=2\mathcal{P}\int_0^\infty d\bar{z}\frac{\bar{z}^2 I_d(\bar{z},x)}{z^2-\bar{z}^2}. \quad (25a)$$

In the low-density limit for which $x=\omega_{p0}/\omega_0\to 0$,

$$P_d(z,0)=-z^{-2}\pi\{(1+|z|)^{3/2}+(1-|z|)^{3/2}\theta(1-|z|)-2\}. \quad (25b)$$

The function $P_d(z,x)$ has been plotted in Fig. 5 as a function of $z=\omega/\omega_0$ for various values of $x=\omega_{p0}/\omega_0$. Note that the curves of Fig. 5 do not display the sharp cusps of the corresponding polar-phonon curves of Fig. 3. This reflects the fact that the function $I_d(z,x)$ of Fig. 4 rises much less steeply at the absorption threshold than does the function $I_p(z,x,R^2)$ of Fig. 2.

Just as we did in Eq. (15) ff. for the function $P_p(z,x,R^2)$, we can view the function $P_d(z,x)$ and its coefficients in (24) as a phonon correction to the electron mass as it appears in ω_{p0}^2. From $P_d(0,0)=-3\pi/4$ we infer the low-energy mass correction $m\to m[1+(E_K^2K^2\omega_0/32\pi m\rho_M\epsilon_\infty)(2m/\hbar\omega_0)^{5/2}]$. As before, screening of the electron-phonon interaction by other electrons ($x=\omega_{p0}/\omega_0>0$) reduces the mass correction below the single-electron value.

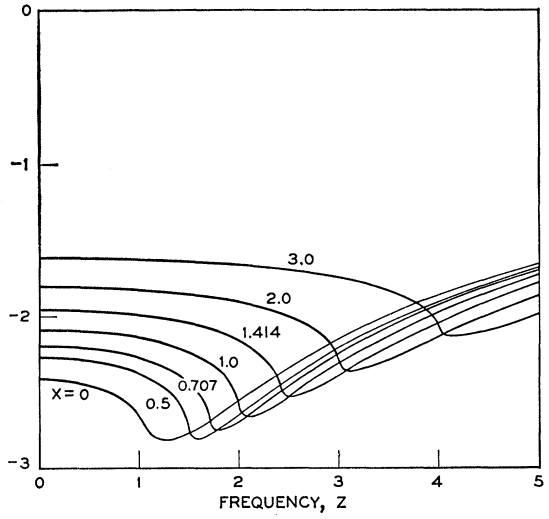

FIG. 5. Deformation-potential-phonon collision-correction function $P_d(z,x)$ as a function of frequency $z=\omega/\omega_0$ for different values of $x=\omega_{p0}/\omega_0$.

IV. RELEVANCE TO EXPERIMENT

Barker[7] and Baer[11] have tentatively attributed small anomalies in the infrared dielectric properties of some polar semiconductors to polar-phonon collision corrections of the type we have discussed in Sec. II. A detailed analysis of these anomalies requires a more complete understanding of the electronic band structure of the materials and, perhaps, extensions to the theoretical results described above. Nevertheless, the available evidence suggests that collision corrections do produce observable modifications in the infrared properties of semiconductors.

Our preceding analysis of collision corrections is incomplete in several important ways. Only first-order, albeit dynamically screened, collisions have been considered; higher order multiple-collision corrections will be important when phonon-electron interactions are strong (e.g., $\alpha\gtrsim 2$ in Sec. II). The Fermi energy $\hbar\omega_F$ has been assumed small relative to $\hbar\omega_{p0}$; while this is valid for some systems, it is generally invalid in materials with $\epsilon_\infty\gg 1$ and $m/m_e\ll 1$ (e.g., GaAs). Finally, only materials with a single active optical-phonon branch, a constant isotropic electron mass, and a single conduction-band valley have been considered, whereas many important materials are more complicated (e.g., $SrTiO_3$ and $BaTiO_3$). We postpone the treatment of these refinements to later papers. From the work[2] of Tzoar we can anticipate, however, that the displaced thresholds (10) and (22) will be conspicuous only if $\omega_{p0}\gg\omega_F, \omega_0$.

In Table I are listed parameters typical of three single-valley polar materials—GaAs, CdS, and ZnO. Using these parameters with Figs. 2 and 3, we can estimate the magnitude of the polar-phonon collision corrections of Eqs. (8) and (13). For example, for a fictitious material not too different from ZnO for which $\alpha=1$ and $R^2=0.5$, we find for $x\lesssim 1$ that the effective-mass correction in the real part of Eq. (13) can be of the order of 30% for $\omega\sim\omega_{l0}$, a fact which must be taken into account in estimating an electron effective mass from reflectivity spectra. Reflectivity spectra computed

TABLE I. Effective masses, dielectric constants, polar coupling constants, and frequencies[a] of some single-valley polar semiconductors.

						$n=6.97\times10^{16}$ cm^{-3}			
	m/m_e	ϵ_∞	ϵ_0	α	ω_{l0}(cm^{-1})	ω_{p0}(cm^{-1})	ω_F/ω_{p0}	$x=\omega_{p0}/\omega_{l0}$	$R^2=\epsilon_\infty/\epsilon_0$
GaAs	0.08	10.9	12.5	0.065	288	84.6	1.75	0.29	0.87
CdS	0.2	5.24	9.19	0.69	306	77.1	0.51	0.25	0.57
ZnO	0.3	4.0	8.15	0.95	591	65.8	0.37	0.11	0.49

[a] Frequencies ω are quoted in wave numbers. In the formulas of the text angular frequencies in rad/sec are required. The conversion factor is $2\pi c=6\pi\times10^{10}$ rad cm/sec.

[11] W. S. Baer, Phys. Rev. 144, 734 (1966).

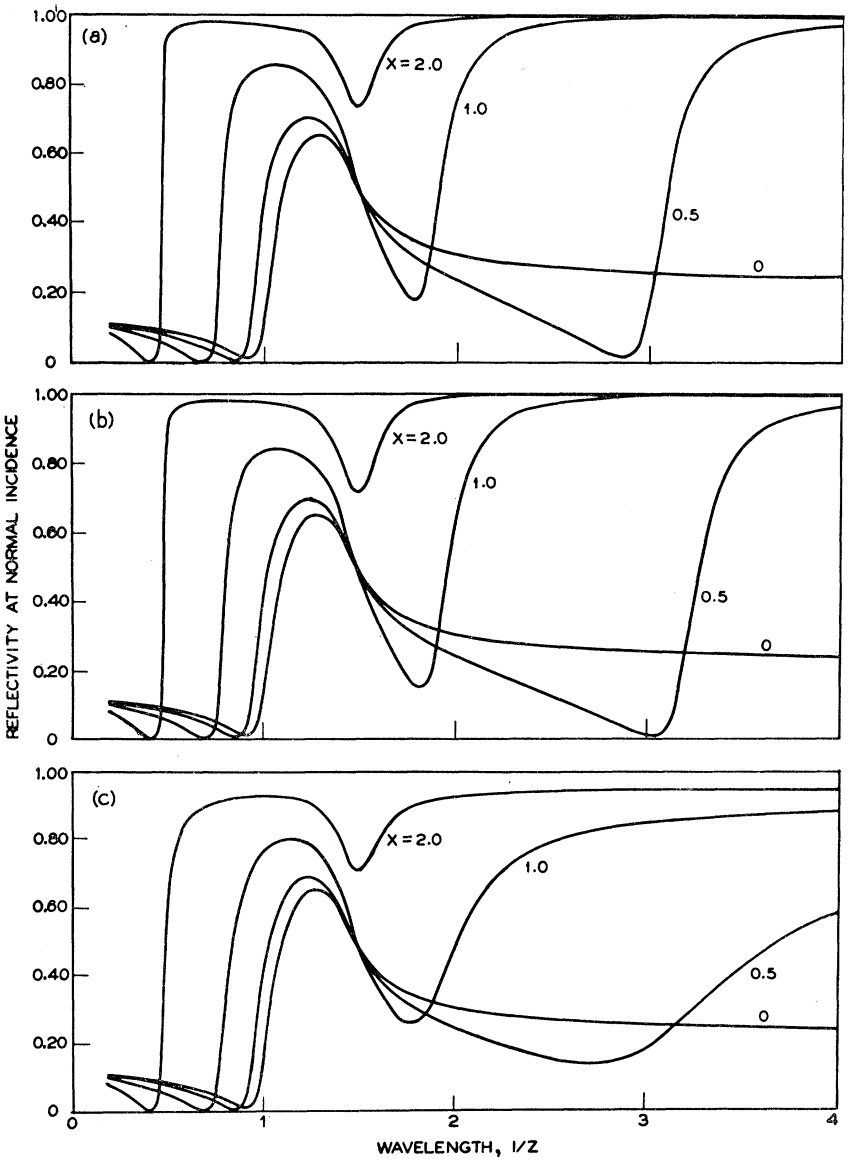

FIG. 6. Reflectivity of a polar crystal at normal incidence as a function of wavelength $1/z=\omega_{l0}/\omega$ for different values of $x=\omega_{p0}/\omega_{l0}$. The plotted reflectivity is $R=|[\epsilon(\omega)^{1/2}-1]/[\epsilon(\omega)^{1/2}+1]|^2$, where $\epsilon(\omega)$ is given by Eq. (13). In all examples, the phonon damping parameter $\gamma=0.05\ \omega_{l0}$ and the dielectric constants $\epsilon_\infty=4$, $\epsilon_0=8$. The polar-phonon coupling parameter α and the collision frequency ν_c are (a) $\alpha=0$, $\nu_c=0$; (b) $\alpha=1$, $\nu_c=0$; and (c) $\alpha=1$, $\nu_c=0.1\omega_{l0}$. Case (a) obtains when all high-frequency collision effects are neglected. The case (not shown) for which $\alpha=0$ and $\nu_c=0.1\omega_{l0}$ differs from (c) in much the same way as (a) differs from (b).

from Eq. (13) have been indicated for this same material in Fig. 6 for a range of carrier concentrations ($x=\omega_{p0}/\omega_{l0}$ is proportional to $n^{1/2}$). In Fig. 6(a) all collision corrections are absent. In Fig. 6(b) the high-frequency one-phonon corrections are included. Their most conspicuous effect is to shift the long-wavelength "plasma" resonance to longer wavelengths through the polaron effective-mass correction already noted. Changes at shorter wavelengths in the neighborhood of the absorption threshold (10) are also present but less conspicuous. The system of Fig. 6(c) differs from that of Fig. 6(b) by the additional inclusion of Drude collisions.

Little is known about the strength of the optical-mode deformation potential E_K or about the relevance to measured spectra of the deformation-potential collision corrections of Eqs. (18) and (24).

ACKNOWLEDGMENTS

The derivation of the single-collision results described above was stimulated by conversations with A. S. Barker and W. S. Baer concerning their experimental observations, and I wish to acknowledge their helpful participation. I am also grateful for their advice in selecting the "typical" parameters listed in Table I.